European Journal of Cardio-Thoracic Surgery 52 (2017) 1090–1097
doi:10.1093/ejcts/ezx203 Advance Access publication 15 June 2017

ORIGINAL ARTICLE

Cite this article as: Shah P, Romagnoni C, Jaworek M, Lucherini F, Contino M, Menkis A *et al*. A novel system for the treatment of aortic annular dilation: an *ex vivo* investigation. Eur J Cardiothorac Surg 2017;52:1090–7.

A novel system for the treatment of aortic annular dilation: an *ex vivo* investigation

Pallav Shah[a,b], Claudia Romagnoni[c,d], Michal Jaworek[c,e], Federico Lucherini[c,e], Monica Contino[c,d], Alan Menkis[a,b], Guido Gelpi[c,d], Gianfranco B. Fiore[c,e], Carlo Antona[c,d,f] and Riccardo Vismara[c,e,*]

[a] Department of Surgery, Max Rady College of Medicine, University of Manitoba, Winnipeg, MB, Canada
[b] Cardiac Sciences Program, St. Boniface Hospital, Winnipeg, MB, Canada
[c] ForcardioLab, Fondazione per la Ricerca in Cardiochirurgia ONLUS, Milan, Italy
[d] Department of Cardiovascular Surgery, 'Luigi Sacco' General Hospital, Milan, Italy
[e] Dipartimento di Elettronica, Informazione e Bioingegneria, Politecnico di Milano, Milan, Italy
[f] Università degli Studi di Milano, Milan, Italy

* Corresponding author. Dipartimento di Elettronica, Informazione e Bioingegneria, Politecnico di Milano, p.za L. da Vinci 32, 20133 Milano, Italy. Tel: +39-02-23994142; e-mail: riccardo.vismara@polimi.it (R. Vismara).

Received 3 March 2017; received in revised form 15 May 2017; accepted 21 May 2017

Abstract

OBJECTIVES: The main reason for aortic repair failures is recurrent annular dilatation. The fibrous portion of left ventricular outflow tract dilates. A novel device was designed to tackle this problem.

METHODS: The device consists of an internal ring applied at the aortic annulus plus an external flexible band at the level of the aortic root. The internal ring has a semi-rigid portion (40%, placed at ventriculo-arterial junction) and a flexible portion to allow it to conform along the curves of the non-coronary/right coronary leaflet and right coronary/left coronary leaflet commissures. The external band acts as a reinforcement to the internal ring. A pulsatile mock loop capable of housing porcine aortic valve was used. Working conditions were 60 bpm of heart rate, 75 of stroke volumes and 120–80 mmHg of simulated pressure. Mean gradient, effective orifice area, annular diameter, coaptation height and length were recorded on 11 aortic root units (ARUs). High-speed video and standard echocardiographic images were also recorded. All data were acquired in the following conditions: (i) basal (untreated ARU); (ii) pathological condition (left coronary/non-coronary triangle was dilated by suturing an aortic patch); and (iii) ARU treated with the device.

RESULTS: Gradients and effective orifice area were respectively 0.9 ± 0.64 mmHg and 3.1 ± 0.7cm^2 (pathological) and 3.7 ± 1.1 mmHg and 1.5 ± 0.2cm^2 (treated, $P < 0.05$). Left coronary/non-coronary diameter decreased from 2.4 ± 0.2 cm (pathological) to 2.0 ± 0.2 (treated, $P < 0.05$). Coaptation length and height were fully restored to basal values following treatment. Visual inspection showed proper dynamics of the leaflet, confirmed by high-speed video and echocardiography.

CONCLUSIONS: The device allowed for restoring physiologic-like coaptation in the experimental model, without inducing clinically relevant worsening of the haemodynamics of the treated ARU.

Keywords: Aortic valve • Aortic valve repair • Annuloplasty ring

INTRODUCTION

Aortic valve (AV) repair is considered as an alternative to AV replacement for pure aortic regurgitation (AR) [1, 2]. In patients with AR, the degree of ventriculo-aortic junction dilatation correlates with the severity of AR resulting from improper leaflet coaptation [3]. AV repair is not widely performed due to difficulties to treat leaflet prolapse, annular dilatation, STJ dilatations, ascending aorta dilatation and combined disease in a complex structure, as it is the aortic root unit (ARU) [4]. Mid-term results of AV repair are promising, but recurrence of AR has been reported at times related to dilatation of ventriculo-arterial junction (VAJ) not only in valve preserving but also in primary AV repair procedures [5–9]. In mitral repair surgery, prosthetic annuloplasty ring in addition to reparative procedure is a well-established concept [10].

The current annuloplasty in use are the following: (i) subcommissural annuloplasty, as advocated by Cabrol *et al.* [11], which involves constriction of interleaflet triangle. It is a simple and an effective technique, but does not touch the problem of annular dilatation resulting in recurrent annular dilatation and reoperation [6, 9]; (ii) external ring by Lansac *et al.* [12]: this approach has reported acceptable 5-year results but has not gained

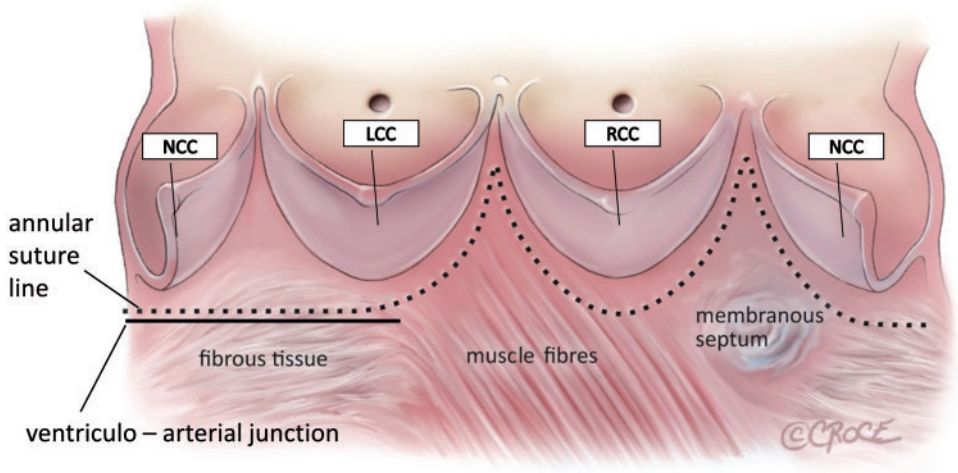

Figure 1: Internal suture line for the aortic annular system. NC: non-coronary leaflet; LC: left coronary leaflet; RC: right coronary leaflet.

popularity as external rings are difficult to place at the annular plane along the muscular ridge of the right coronary (RC) leaflet; and (iii) Rankin ring [13]: acceptable 2-year follow-up was published. This ring has elliptical base geometry and subcommissural posts, giving it a crown-shaped appearance similar to normal AV. The concept is based on the fact that all 3 intercommissural triangles are equal, which is not always the case. In particular, in bicuspid valves, the annulus is asymmetrically dilated and deeper at the aortomitral curtain, rendering insertion of this ring not ideal. Similar issues exist when this approach is applied to Marfan patients [14].

None of these approaches is conceived considering the heterogeneous biomechanical properties of the aortic annulus (defined as the virtual basal plane along the nadir of the 3 leaflets), which reflects on asymmetrical dilation. The dilatation occurs along the fibrous portion of the left ventricular outflow tract. The fibrous portion comprises the following: (i) interleaflet triangle along non-coronary (NC)/left coronary (LC) leaflets and the area of fibrous continuity between the leaflets of the aortic and mitral valves or VAJ; (ii) the membranous portion between the RC and NC leaflets that, in continuity with the right fibrous trigone, forms the 'central fibrous body'. They are positioned between the semilunar hinges of the leaflets as they extend to insert to the sinutubular junction. Muscular portion typically does not dilate. So, in most of the pathologies like Marfan, bicuspid valve, annulo-aortic ectasia and other connective tissue disorders, the annular dilatation will be asymmetrical, unless in case of very advanced disease [15].

Ideally, an annular system for treating aortic annular dilation should be designed considering the following: (i) the annular dynamics of contractions and relaxations during the cardiac cycle; (ii) the 3D shape of the aortic annulus; (iii) the anatomical–functional constrains (e.g. the conduction bundle between the RC and NC leaflets); and (iv) the differences in annular tissues in terms of composition (fibrous or muscular).

In this paper, a novel aortic annular system (AAS) had been designed, taking into account the above-presented issues. The purpose of the study was to evaluate the effect of the device implantation on AV functioning and haemodynamics. For that purpose, the device was implanted in dilated swine aortic roots. Fluid dynamics and echocardiographic data pre- and post-implantation were acquired and compared.

MATERIALS AND METHODS

Design principles of the device

The AAS consists of an internal ring designed to be applied at the aortic annular level, plus an external flexible band to be applied at the level of the aortic root. The internal ring is oval, with a semi-rigid 40% part of its perimeter designed to be placed at the VAJ or the plane of mitral–aortic continuity (Fig. 1). The remaining portion of the ring is flexible and designed to be placed at the muscular and membranous portion of the annulus. The flexible portion of the ring features an extra 5% length to the normal 60% of its perimeter to allow for it to conform along the curves of NC/RC leaflets (membranous) and RC/LC leaflets commissures (muscular) (Fig. 1, dotted lines). The external band is intended as a reinforcement to the internal ring. These dimensions are based on how each portion is represented in the human left ventricular outflow tract [16, 17].

Manufacturing details

The semi-rigid portion of the ring consists of a 0.8-mm (0.030″) diameter MP35N wire embedded within a silicone elastomer with a shore hardness of 30 A. The flexible portion is made entirely of silicone elastomer. The whole ring is encased within a polyethylene terephthalate circular knit tube. The band is made up of a 5.6-mm (0.219″)-wide polyethylene terephthalate knit fabric. Eleven rings with a diameter of 21 mm (0.827″) were used for this study.

The ring was secured to a plastic holder, which snapped onto a stainless steel handle to facilitate positioning (Fig. 2). The ring was located below the aortic leaflets, and the band was positioned opposite to the ring and external to the aortic root. The ring, band and aortic tissue were attached together with sutures. Parts were manufactured at BOMImed Inc. (Winnipeg, MB, Canada).

Suturing technique

The suturing technique scheme is shown in Fig. 3. The fibrous portion of the annulus lies below the NC/LC leaflets, the muscular portion below the LC/RC leaflets and the membranous

portion below the RC/NC leaflets. The semi-rigid (grey) portion of the ring is placed at the VAJ in a straight line to allow the maximum annular reduction, while the flexible (white) portion goes up along the commissures of NC/RC and LC/RC leaflets to avoid membranous septum and away from muscular septum (Fig. 1). In the semi-rigid portion of the ring, the U sutures were 2 mm wide at ring, wider apart at the fibrous annulus to allow annular reduction and went back to 2 mm on the external band. In the flexible portion, sutures were 2 mm wide in ring, annulus and band. The external band was divided twice at the level of the coronary ostia. The ring was lowered to the annular plane prior to removing the holder, and then the sutures were passed through the band. The sutures were first tied at the fibrous annulus and nadir of the RC leaflet and then the rest of the sutures were tied.

Figure 2: Complete assembly of the device with the holder.

Experimental apparatus

A pulsatile mock loop capable of housing swine ARUs was used for the experimental model [18, 19]. Figure 4 reports a schematic of the mock loop. The pulsatile flow was pushed by the pump ***d*** through the ARU sample ***a***. The flow entered the afterload ***e*** that mimic the systemic input impedance, to guarantee a physiologic-like systemic pressure to the sample ***a***. The fluid passed from ***e*** to the atrial bath ***b*** and returned to the ventricle ***c*** through a service valve (in red) acting as mitral valve, thus closing the hydraulic ring. The experimental apparatus allowed for measuring and recording pressure downstream to and upstream from the ARU (p_1 and p_2 respectively) as well as the flow rate downstream from the ARU (Q).

The swine ARUs were selected according to the size of the AAS (21 mm) available for the study. The ARU sizing procedure was

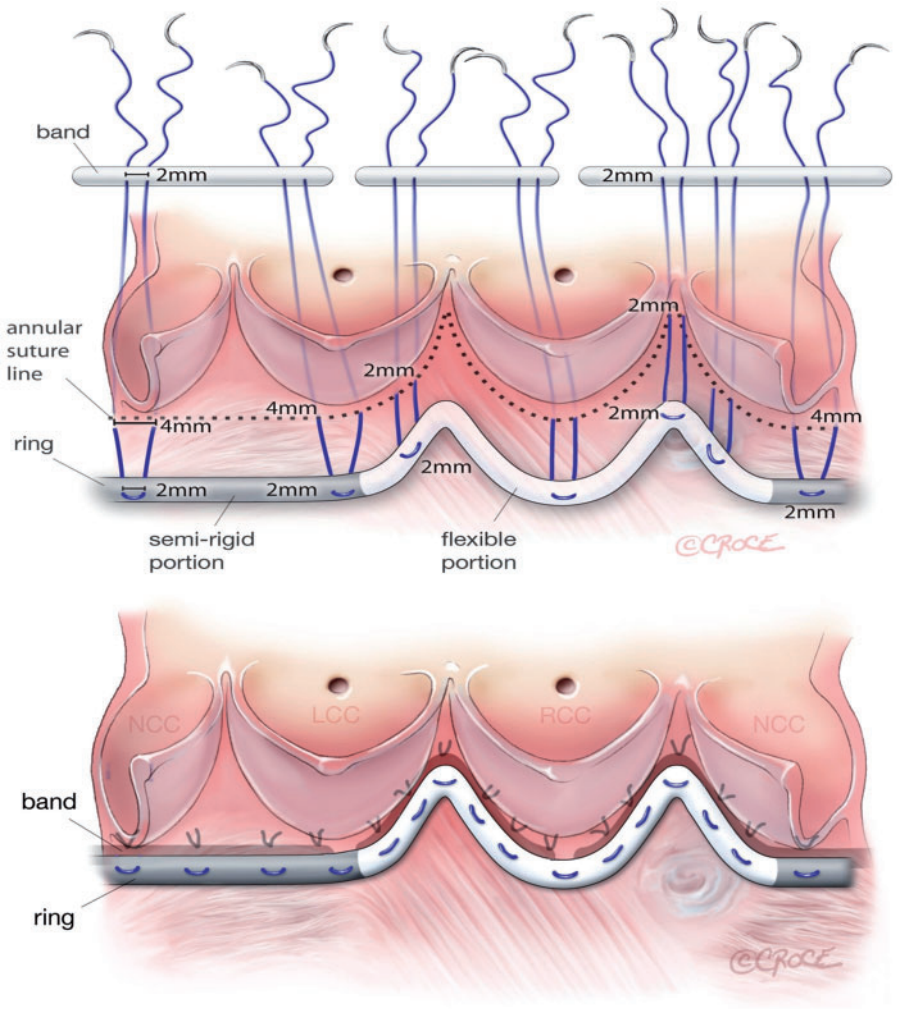

Figure 3: The suturing technique is shown. The flexible portion of the internal ring is in white, while the semi-rigid part is in grey. NC: non-coronary leaflet; LC: left coronary leaflet; RC: right coronary leaflet.

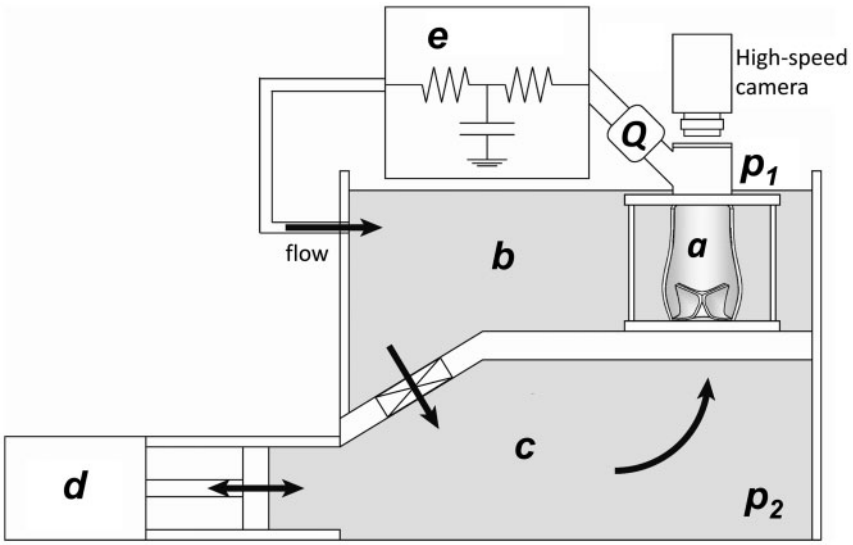

Figure 4: Schematic of the experimental apparatus. ***a***: porcine aortic root unit; ***b***: atrial bath; ***c***: ventricular chamber; ***d***: pulsatile pump; ***e***: systemic input impedance simulator; p_1, p_2: aortic and ventricular pressure ports, respectively; ***Q***: flowmeter probe.

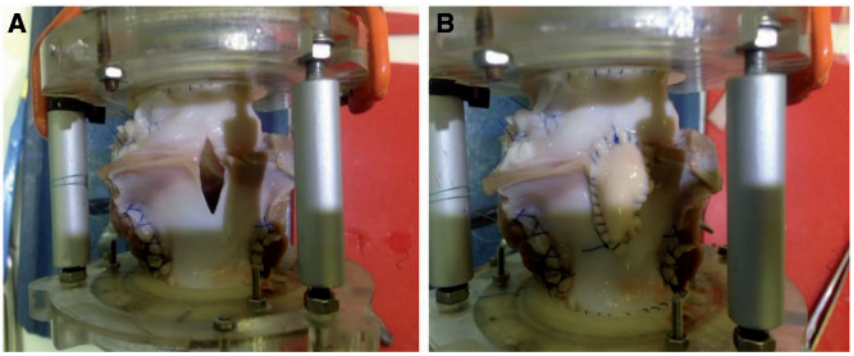

Figure 5: Surgical preparation of the dilated aortic root. (**A**) A surgical cut (about 15-mm axial length) was performed in correspondence to the left coronary and non-coronary intercommissural triangle. (**B**) A patch obtained from the aorta was sutured in correspondence to the cut. Maximum circumferential dimension of the patch was approximatively 10 mm, to allow for the root to dilate.

comparable to the sizing procedure adopted in the operating room and was performed by experienced surgeons.

Each ARU was housed in the test section of the mock loop in basal condition and tested. Then, the pathological condition and the treated condition were obtained in each ARU. In each of these 2 configurations, the ARU was tested again, in the same mock loop settings, and data were acquired.

Pathological model for aortic valve dilatation

The strategy to get the pathological model of swine ARU was taken from the literature [20]. A 15-mm-long cut in the ARU axial direction was performed in correspondence with the intercommissural triangle between LC and NC leaflets (Fig. 5A). The cut was from the top of the NC/LC leaflet commissure to the anterior mitral leaflet. A rhomboidal patch of tissue was harvested from the porcine aorta and sutured according to the cut (Fig. 5B). Approximate dimensions of the patch were 10 mm (ARU circumferential direction) and 15 mm (axial direction), to allow for the sample to dilate circumferentially.

Test methods and procedure

Eleven AASs of size 21 mm were tested in selected swine ARUs. The size of the annulus was measured by standard St Jude Medical aortic sizers. The AASs were implanted by a cardiac surgeon. A single-operator implanting strategy was adopted to avoid inter-operator bias.

Two kinds of tests (A and B, respectively) were performed. Tests A were designed to investigate the effect of AAS implantation on the ARUs in terms of fluid dynamic alteration and coaptation/function of the AV. Tests B were designed to investigate the fluid dynamic performance of the treated ARUs when tested at increasing SVs.

Test A. The following conditions were tested in sequence for each ARU:

a. Basal condition. The ARU was tested in untreated condition so as to record the main biomechanical parameters in physiologic-like conditions.

b. Pathological condition. The pathology was simulated in the *ex vivo* ARU model, as described earlier, to have a model of dilated root. The ARU was tested in these conditions.
c. Treated condition. The AAS was implanted in the pathological model of ARU and tests were run again with data acquisition.

Mock loop was set at 60 bpm, with a stroke volume (SV) of 75 ml and a systolic/diastolic systemic pressure of 120/80 mmHg. In each condition, the pressures upstream from and downstream to the ARU, and the flow rate across the ARU were acquired. From the raw experimental data, the following measurements were obtained and compared in the 3 conditions a, b and c:

- CO: cardiac output, l/min: mean flow rate evaluated from the Q measured downstream from the ARU.
- Δp_{max}, mmHg: maximum systolic pressure drop (from p_1 and p_2).
- Δp_{mean}, mmHg: mean systolic pressure drop (from p_1 and p_2).
- EOA, cm^2: effective orifice area, evaluated as follows [4]:

$$EOA = \frac{Q_{rms}}{k\sqrt{\Delta P_m}},$$

where Q_{rms} (l/min) was the mean square root of the systolic flow rate, ΔP_m (mmHg) the mean systolic pressure drop across the sample and k a conversion factor ($k = 3.1$ to yield the EOA in square centimetre).

Echocardiographic images were acquired to evaluate the morphological differences between basal, pathological and treated conditions in terms of a geometric orifice area (GOA), coaptation height, coaptation length and aortic annulus. The geometric orifice area was evaluated in short axis, at the maximum valve opening, measuring the area of the opening orifice. Long-axis images of the 3 coaptation surfaces (NC/LC, NC/RC and RC/LC leaflets) were acquired and, for each of them, the annulus (defined as the distance between the 2 leaflets nadir), the coaptation height (i.e. the distance between the tip of the coaptation and the annular plane) and the coaptation length (the distance in which the 2 leaflets coaptation) were evaluated. All echo evaluations were performed by the same operator.

Values were averaged over 10 simulated cardiac cycles and were reported as mean and standard deviation. A total of 11 ARUs were tested in this series.

Test B. Of the 11 ARUs, 7 were tested, only in treated conditions (*c*), with the mock loop set to 60 bpm, 120/80 mmHg of systemic pressure and the SV set at 55 ml, 75 ml and 95 ml. The purpose of these tests was to evaluate the hydrodynamic performance of the device simulating different patient/device mismatch. In these experimental conditions, the CO, p_{max}, and p_{mean} were evaluated.

Statistical analysis

Ten consecutive simulated cycles in each experimental point were analysed to obtain fluid dynamic data for each tested experimental point. Overall data were presented as mean ± standard deviation following the assessment of normal distribution. Statistical significance ($P < 0.05$) was evaluated using repeated-measures analysis of variance and with Bonferroni's *post hoc* test.

RESULTS

Pooled data for the Tests A and B are reported below.

Test A

Fluid dynamics. Main fluid dynamic findings are reported in Fig. 6 (means with standard deviation as error bars). The CO slightly decreased following ARUs enlargement (from 3.65 ± 0.21 l/min, basal, to 3.30 ± 0.30 l/min, pathological, $P < 0.05$). Annular enlargement did not change the maximum nor mean systolic pressure drop across the ARU, as expected. The implantation of the AAS induced statistically significant ($P < 0.05$) increment of p_{max} (from 17.30 ± 1.7 mmHg, pathological, to 21.11 ± 4.6 mmHg post-treatment) and p_{mean} (from 0.94 ± 0.43 mmHg to 3.65 ± 1.07 mmHg post-treatment). EOA decreased from 5.37 ± 1.21 cm^2 to 2.62 ± 0.34 cm^2 following the treatment ($P < 0.05$).

Echocardiographic data. Echocardiographic data described the variation of coaptation geometry when passing from the physiologic ARUs to the pathological and to the treated ARUs (Fig. 7). The pathological model induced a statistically signficant reduction of coaptation length as well as copatation height in the ARUs, regardless of the couple of leaflets used as a reference for the echographic evaluation. The treatment allowed for a complete recovery of these quantities to the values recorded in basal ARUs.

With regard to annular diameter, the annulus enlarged in LC-NC direction (pathological) compared to basal state ($P < 0.05$). This enlargement returned to basal following AAS treatment. The geometric orifice area decreased from 4.83 ± 0.65 cm^2 (pathological) to 3.85 ± 0.76 cm^2 following treatment ($P < 0.05$).

Test B

These tests (Fig. 8) at different SVs were performed only on the treated ARUs. The CO increased from 2.43 ± 0.29 mmHg (SV = 55 ml) to 4.83 ± 0.46 ml (SV = 95 ml), $P < 0.05$. The maximum pressure increased from 13.27 ± 1.26 mmHg (minimum SV) to 23.33 ± 1.47 mmHg (maximum SV, $P < 0.05$), and the mean systolic pressure increased from 0.73 ± 0.42 mmHg (minimum SV) to 5.70 ± 0.92 mmHg (maximum SV, $P < 0.05$).

DISCUSSION

In this work, a novel device for the treatment of aortic annular dilation is presented. The device consisted of an internal ring oval in shape. A semi-rigid portion of the ring was placed at the VAJ to reduce, prevent further dilatation and give stability. A flexible portion of the ring was designed to confer along the curves of NC/RC and LC/RC leaflets to protect the conduction bundle and allow dynamic motion of the annulus during cardiac cycle. Dedicated *in vivo* tests will allow for an experimental assessment of the residual risk of atrioventricular block associated with this design. A flexible external band was intended to reinforce and increase the strength of the entire system. Tested in an *ex vivo* experimental set-up, the device allowed for a full recovery of the leaflet coaptation, without inducing clinically relevant alteration to the AV functioning and haemodynamics.

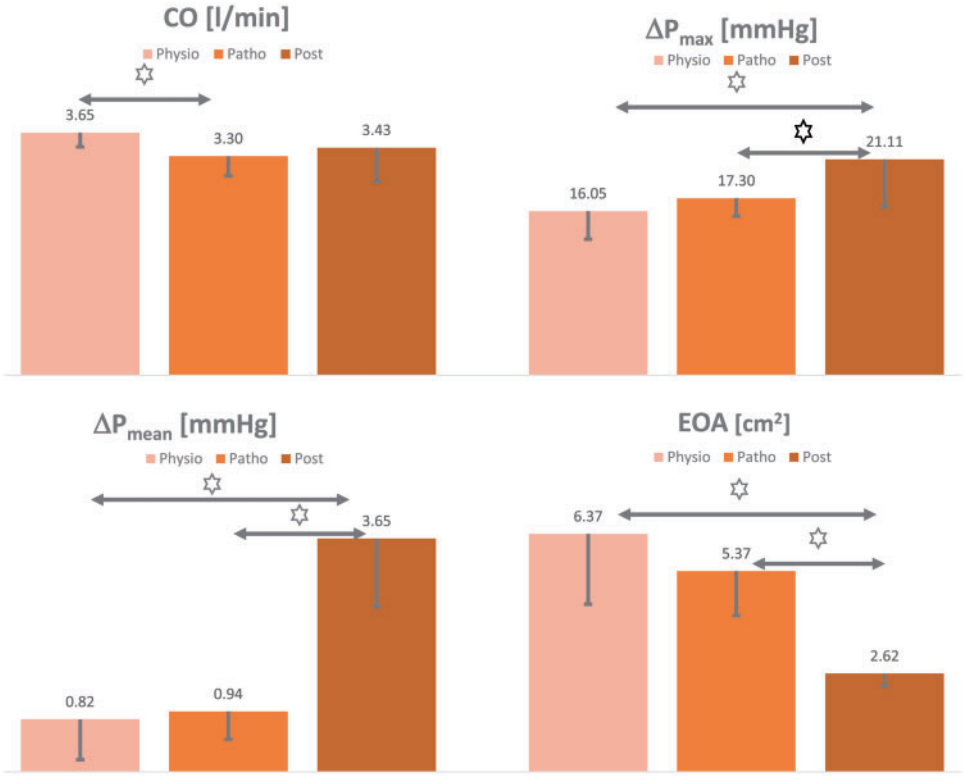

Figure 6: Hydrodynamic findings: cardiac output (CO, l/min), maximum and mean systolic pressure drop (p_{max} and p_{mean} mmHg) and effective orifice area (EOA, cm^2) measured in simulated physiological, pathological and post-treatment conditions. Mean ± SD (bars) evaluated over 11 samples are reported. Star indicates statistical significance ($P < 0.05$).

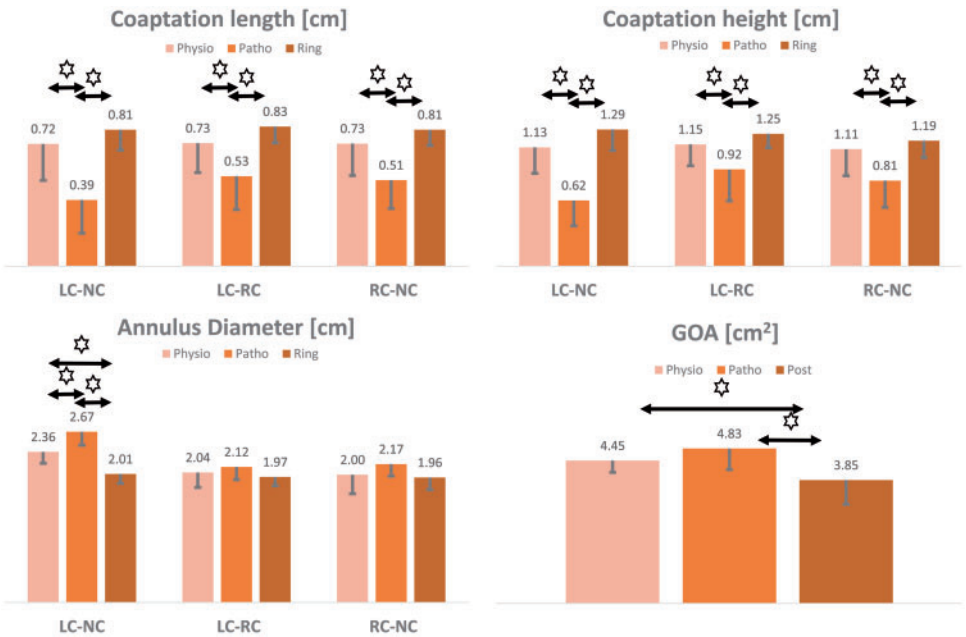

Figure 7: Echocardiographic main findings. Coaptation length and height are evaluated in simulated physiological, pathological and treated conditions between the (LC-NC), LC-RC and RC-NC leaflets. Mean ± SD (bars) evaluated over 11 samples are reported. Star indicates statistical significance ($P < 0.05$). LC-NC: left coronary/non-coronary; LC-RC: left coronary/right coronary; RC-NC: right coronary-non coronary; GOA: geometric area orifice.

An established experimental approach was adopted to assess primarily the impact of the implantation of the novel device on valve haemodynamics. Indeed, it is well recognized that an increase in pressure drop, following treatment, is associated with valve replacement and as well with AV annuloplasty [18, 19]. Following the assessment of the haemodynamic performance of the treatment, the pathological model of the ARU allowed us to assess the potential of the applied device in restoring the correct leaflet coaptation length and height in an experimental model that represents the immediate postoperative scenario.

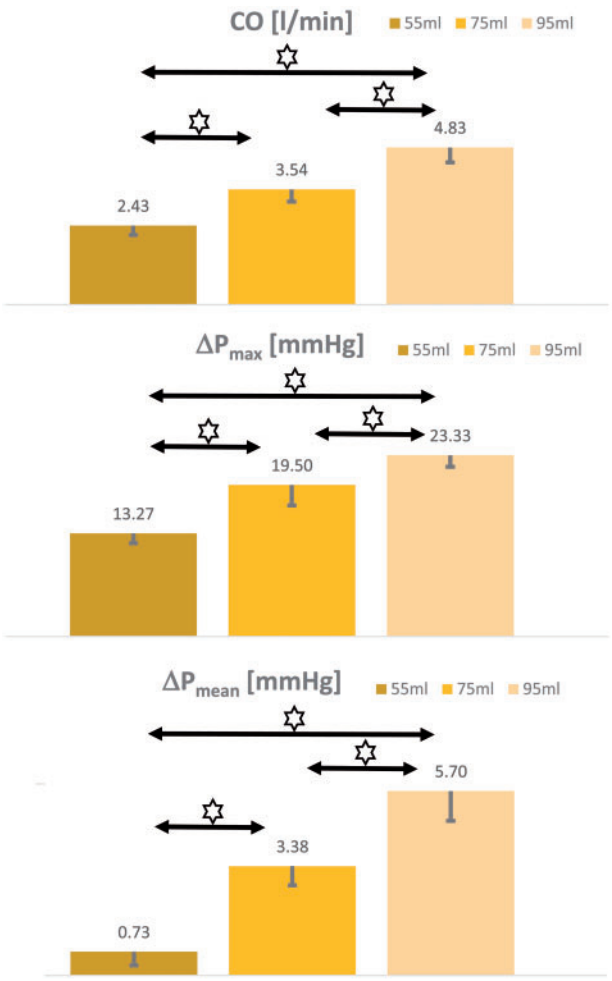

Figure 8: Hydrodynamic findings in post-treatment samples evaluated for different imposed stroke volumes (55, 75 and 95 ml): cardiac output (CO, l/min), maximum and mean systolic pressure drop (p_{max} and p_{mean} mmHg). Mean ± SD (bars) evaluated over 7 samples are reported. Star indicates statistical significance ($P < 0.05$).

Ex vivo test methodology

The proposed approach to obtain dilated swine ARUs was taken from the literature [20]. The methodology allowed to get a statistically significant dilation of the interleaflet triangle between the LC and the NC leaflets, coherently with the triangle that was enlarged in this experimental model. This resulted in significantly reduced coaptation length and height. The model did not induce AR and thus did not cause significant alteration in CO with respect to the physiological conditions. This means that the imposed dilation did not allow complete loss coaptation between the leaflets.

Haemodynamic findings

Following treatment, a significant increase in both maximum and mean systolic pressure drops with respect to untreated and pathological conditions was measured. This means that the internal ring induced a degree of interference with the haemodynamics. Of note, the absolute values of the pressure drop never reached clinically relevant values, and where lower, with respect to data reported in the literature concerning *in vitro* tests of state-of-the-art bioprostheses designed for the same size [19]. Moreover, it should be considered that a physiological SV for 21 mm ARU should be between 55 ml and 75 ml [19], when a mean pressure increase ranging from 0.73 ± 0.42 mmHg to 3.38 ± 0.59 mmHg was recorded. The maximum tested SV of 95 ml represented a simulation of mismatch between the treated ARU and the patient, and the recorded mean pressure drop in these conditions (5.70 ± 0.92 mmHg) was not of clinical relevance. The EOA decreased following treatment: basal values were similar to reports from the literature and values for treated ARUs were similar to data reported for VAJ annuloplasty [18] and bioprostheses [19] evaluated in the same experimental scenario.

Echocardiographic findings

Following the treatment of the pathological ARUs, the coaptation geometric parameters were restored to their original physiological values. In particular, no statistically significant differences were obtained in coaptation lengths and heights between basal and treated ARU. Of note, the coaptation lengths were higher in treated model with respect to the basal state. This increased coaptation could provide a functional reserve that might correlate with a stable valve functioning over the time.

Limitations

The proposed methodology suffered from the limitations of the *ex vivo* approaches. First, it allowed for the investigation of a scenario that replicates the acute postoperative conditions. Thus, we assessed that the proposed treatment did not alter the valve haemodynamics and functioning in the treated model, with a proper coaptation of the valve. Mid- to long-term outcomes require specific *in vivo* investigations to assess implant durability and the associated risk of leaflet damage due to the internal ring placement. A second limitation of the study relies in the fact that the ARU lost all its muscle activity in the experimental set-up. This muscle activity induces ventriculo-aortic junction shape alteration during the cardiac cycle. These alterations could in turn have an effect on the haemodynamics and leaflet coaptation. Another limitation of the study relies in the anatomical differences between swine and human aortic root. Despite the swine model is often used in *ex vivo* studies, some anatomical peculiarities are a limiting factor in this study. For example, the design of the pathological model with only NC/LC intercommissural triangle dilation replicates a specific model of annulo-aortic ectasia. In the real settings, often the RC/NC intercommissural triangle also dilates. The swine aortic root, which has a pronounced muscular shelf in this zone, did not allow for a controllable *ex vivo* dilation with the surgical patch adopted in this work. Both these limitations could be addressed in targeted tests on animal models.

CONCLUSIONS

The work demonstrates in an *ex vivo* acute experimental set-up that the novel device does not induce clinically relevant impairment to the haemodynamics and can restore correct coaptation length and height in dilated aortic annulus. It did not affect valve motion on visual inspection, high-speed video or on echocardiography. This study can be considered a promising starting point for further evaluation of the approach, aimed at assessing treatment durability and efficacy over the time.

Funding

This work was supported by the Industrial Research Assistance Program (IRAP), National Research Council, Canada; Commercialization Support for Business program (CSB), Government of Manitoba Initiative; Fondazione per la Ricerca in Cardiochirurgia ONLUS, Milan, Italy; and European Commission, Horizon 2020 framework through the MSCA-ITN-ETN European Training Networks (project number 642458).

Conflict of interest: none declared.

REFERENCES

[1] Aicher D, Fries R, Rodionycheva S, Schmidt K, Langer F, Schafers HJ. Aortic valve repair leads to a low incidence of valve-related complications. Eur J Cardiothorac Surg 2010;37:127–32.

[2] Boodhwani M, de Kerchove L, Glineur D, Poncelet A, Rubay J, Astarci P *et al*. Repair-oriented classification of aortic insufficiency: impact on surgical techniques and clinical outcomes. J Thorac Cardiovasc Surg 2009;137:286–94.

[3] Padial LR, Oliver A, Sagie A, Weyman AE, King ME, Levine RA. Two-dimensional echocardiographic assessment of the progression of aortic root size in 127 patients with chronic aortic regurgitation: role of the supra-aortic ridge and relation to the progression of the lesion. Am Heart J 1997;134:814–21.

[4] Vismara R, Leopaldi AM, Mangini A, Romagnoni C, Contino M, Antona C *et al*. In vitro study of the aortic interleaflet triangle reshaping. J Biomech 2014;47:329–33.

[5] Kunihara T, Aicher D, Rodionycheva S, Groesdonk H-V, Langer F, Sata F *et al*. Preoperative aortic root geometry and postoperative cusp configuration primarily determine long-term outcome after valve-preserving aortic root repair. J Thorac Cardiovasc Surg 2011;143:1389–95.

[6] Aicher D, Kunihara T, Abou Issa O, Brittner B, Gräber S, Schäfers HJ. Valve configuration determines long-term results after repair of the bicuspid aortic valve. Circulation 2011;123:178–85.

[7] Aicher D, Schneider U, Schmied W, Kunihara T, Tochii M, Schäfers HJ. Early results with annular support in reconstruction of the bicuspid aortic valve. J Thorac Cardiovasc Surg 2013;145:S30–4.

[8] de Kerchove L, Jashari R, Boodhwani M, Duy KT, Lengelé B, Gianello P *et al*. Surgical anatomy of the aortic root: implication for valve-sparing reimplantation and aortic valve annuloplasty. J Thorac Cardiovasc Surg 2015;149:425–33.

[9] de Kerchove L, Boodhwani M, Glineur D, Vandyck M, Vanoverschelde JL, Noirhomme P *et al*. Valve sparing-root replacement with the reimplantation technique to increase the durability of bicuspid aortic valve repair. J Thorac Cardiovasc Surg 2011;142:1430–8.

[10] Gillinov AM, Tantiwongkosri K, Blackstone EH, Houghtaling PL, Nowicki ER, Sabik JF 3rd *et al*. Is prosthetic anuloplasty necessary for durable mitral valve repair? Ann Thorac Surg 2009;88:76–82.

[11] Cabrol C, Cabrol A, Guiraudon G, Bertrand M. Treatment of aortic insufficiency by means of aortic annuloplasty. Arch Mal Coeur Vaiss 1966;59:1305–12.

[12] Lansac E, Di Centa I, Sleilaty G, Lejeune S, Khelil N, Berrebi A *et al*. Long-term results of external aortic ring annuloplasty for aortic valve repair. Eur J Cardiothorac Surg 2016;50:350–60.

[13] Mazzitelli D, Fischlein T, Rankin JS, Choi YH, Stamm C, Pfeiffer S *et al*. Geometric ring annuloplasty as an adjunct to aortic valve repair: clinical investigation of the HAART 300 device. Eur J Cardiothorac Surg 2016;49:987–93.

[14] Sievers HH. Aortic annuloplasty ring: coronet or flat or not or what? Eur J Cardiothorac Surg 2012;42:155–6.

[15] Hahm SY, Choo SJ, Lee JW, Seo JB, Lim TH, Song JK *et al*. Novel technique of aortic valvuloplasty. Eur J Cardiothorac Surg 2006;29:530–6.

[16] Ho SY. Structure and anatomy of aortic root. Eur J Echocardiogr 2009;10:i3–10.

[17] Sands MP, Rittenhouse EA, Mohri H, Merendino KA. An anatomical comparison of human, pig, calf, and sheep aortic valves. Ann Thorac Surg 1969;8:407–14.

[18] de Kerchove L, Vismara R, Mangini A, Fiore GB, Price J, Noirhomme P *et al*. *In vitro* comparison of three techniques for ventriculo-aortic junction annuloplasty. Eur J Cardiothorac Surg 2012;41:1117–23.

[19] Tasca G, Vismara R, Fiore GB, Mangini A, Romagnoni C, Pelenghi S *et al*. Fluid-dynamic results of *in vitro* comparison of four pericardial bioprostheses implanted in small porcine aortic roots. Eur J Cardiothorac Surg 2015;47:e62–7.

[20] Scharfschwerdt M, Pawlik M, Sievers HH, Charitos EI. *In vitro* investigation of aortic valve annuloplasty using prosthetic ring devices. Eur J Cardiothorac Surg 2011;40:1127–30.